Waveform Multiplexing for 5G: A Concept and 3D Evaluation

Yeon-Geun Lim*, Taehun Jung*, Kwang Soon Kim†, and Chan-Byoung Chae*
*School of Integrated Technology, †School of Electrical and Electronic Engineering, Yonsei University, Korea
Email: {yglim, taehun.jung, ks.kim, cbchae}@yonsei.ac.kr

***Abstract*—Fifth generation (5G) communication systems include enhanced mobile broadband, massive machine-type communication, and ultra-reliable low-latency communication. To support various 5G applications, researchers have considered multiple scalable subcarrier spacing and transmission time interval (TTI). In this paper, we introduce a concept of *waveform multiplexing* for frequency multiplexing of numerologies. *Waveform multiplexing* consists of different waveforms on subbands with scalable subcarrier spacing and TTI operating on one frequency band. The *Waveform multiplexing* also possesses dynamic cyclic prefix and minimum guard band, which are the key features for the high spectral efficiency. We verify the performance and the potential of the *waveform multiplexing* using 3-dimensional (3D) ray-tracing based system-level evaluation in a realistic environment and a 3D channel.**

***Keywords*—Multiplexing of numerologies, GFDM, filtered-OFDM, 3D channel model, 3D ray-tracing, system-level simulation, and 5G.**

I. Introduction

In the recent years, researchers have discussed the potential applications of 5th generation (5G) communication. These are serviced along with other requirements for high capacity for enhanced mobile broadband (eMBB), massive machine-type communication (mMTC) connectivity, and ultra-reliable low-latency communication (URLLC) [1]. In the eMBB case, massive multiple-input multiple-output (MIMO), full duplex, non-orthogonal multiple access (NOMA), mm-Wave, and small cell techniques have been extensively studied to enhance spectrum efficiency (bps/Hz), spectrum extension (Hz/cell), and network density (cell/area). MIMO techniques have been evolved from single user MIMO to multiuser MIMO [2]. The authors in [3] investigated performance of massive MIMO system with a lot of antennas at the BS and the large number of the serviced users. A full duplex system doubles its spectrum, and it was already prototyped in real time [4]. NOMA supports users simultaneously on the same resource in either a power domain or a code domain [5], [6]. Hybrid beamforming and electromagnetic-lens antenna techniques have targeted mm-Wave and MIMO [7].

More recently, in trying to meet the various requirements for 5G applications, researchers have considered multiple scalable subcarrier spacing and transmission time interval (TTI). The 3rd Generation Partnership Project (3GPP) has discussed supporting, with various frequency bands, multiple sets of subcarrier spacing and of TTI. The development of techniques to create high-capacity smart phones, an integrated device of applications requiring high data rates, has dominated the mobile market of 4th generation (4G) long-term evolution (LTE) as a killer application. This is expected to continue in 5G. It is quite possible that one of the 5G killer applications could be an integrated device or a central controller of various applications with other requirements, which could be operated on one frequency band. To support such a device, 3GPP has also discussed frequency multiplexing of numerologies. Meanwhile, it has not been determined which waveform will be used and how this system is designed efficiently, yet.

3GPP agreed that new waveform of 5G will be based on orthogonal frequency division multiplexing (OFDM) with filtering or windowing. For example, the authors in [8], [9] proposed filtered OFDM (f-OFDM), which is integrated system of multiple independent OFDM systems with various numerologies based on subband-based splitting and filtering. The out-of-band emissions (OOBE) of each subband can be suppressed by a properly designed baseband finite impulse response (FIR) filter. Because of the suppression of OOBE, guard band usages can be reduced. On each subband, the optimized numerology can be applied to fulfill requirements of a certain type of the services so the various applications could be jointly provided with backward compatibilities.

However, there are still some potential new waveform candidates that could support various applications including nonorthogonal waveforms beyond the initial 5G system. These fulfill low OOBE and have robustness to asynchronous systems. The authors proposed generalized frequency division multiplexing (GFDM) [10], which divides time-frequency resources into blocks that consist of subsymbols and subcarriers. Adopting a circular pulse shaping filter, GFDM does not present filter tails, providing an advantage to low-latency applications. By choosing a well-localized pulse shaping filter, OOBE can successfully be reduced. In the meantime, researchers have studied how to enable filter bank multicarrier (FBMC) to use quadrature amplitude modulation (QAM) and MIMO techniques in 5G [11]. The performance analysis of each waveform has been concentrated on link-level simulation measuring block error rate, OOBE, and overhead due to filter length/cyclic prefix (CP).

To evaluate a system-level performance, researchers have, so far, compared techniques based on analysis in a 2-dimensional (2D) environment. In a conventional outdoor model for system-level simulations, base stations (BSs), one each for three sectors, are placed at regular points following a hexagonal layout with a wrap-around configuration [12]. In practice, BSs and users are located in 3-dimensional (3D) space. As cell sizes have been shrinking with high network

978–1–5386–3873–6/17/$31.00

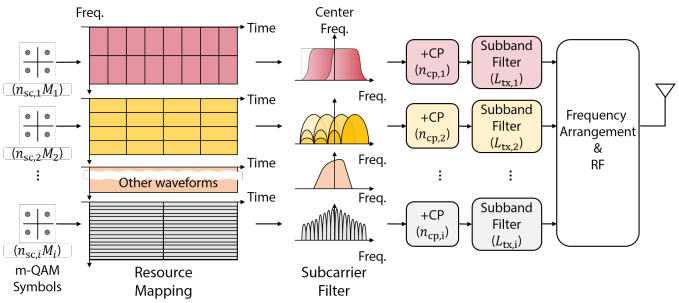

Fig. 1. A block diagram of the proposed *waveform multiplexing* transmitter.

density, it could be important, when evaluating a 5G system, to measure the signal propagation at the elevation angles. The authors in [13] implemented a testbed of a 3D hybrid beamforming algorithm and measured its gain in a small cell. They showed the system-level performance of their algorithm using a 3D ray-tracing tool based on measured data.

In this paper, we present a potential of a system that consists of different waveforms on each numerology. We name this concept *waveform multiplexing*. The *waveform multiplexing* can be more efficiently operated than frequency multiplexing of numerology based on a single waveform. To evaluate how well our *waveform multiplexing* performs, we must jointly combine the link-level results into system-level simulations. We then propose a 3D channel model to evaluate system-level performances more practically by utilizing a realistic digital map. The 3D system-level simulations confirm that the *waveform multiplexing* system outperforms an LTE-based multi-band OFDM system. According to both the OOBE and the time overhead of the waveform candidates, the performances of the proposed *waveform multiplexing* vary in certain environments.

II. Waveform Multiplexing

A. A Concept of Waveform Multiplexing

As mentioned in Section I, 3GPP has discussed the frequency multiplexing of numerologies with the minimum guard band between numerologies. In this paper, we present a *waveform multiplexing* technique as a system of the multiplexing of numerologies operating efficiently. We define *waveform multiplexing* as a subband system having the following characteristics:

• **Multiplexing of Waveforms on Subbands with Scalable Subcarrier Spacing:** One system supports various applications such as eMBB, mMTC, and URLLC, on one frequency band. Each subband consists of different waveforms with various subcarrier spacing. Unlike the f-OFDM system in [8], each subband can utilize different waveforms. This makes one system support multiple sets of symbol duration and TTI, and utilize appropriate waveform set.

• **Dynamic CP:** Thanks to the low OOBE of 5G waveform candidates, the proposed *waveform multiplexing* can optimize a multiband system by employing different CP lengths. Conventional OFDM systems have strictly employed a fixed CP length so as to avoid destroying their orthogonality. The dynamic CP technique has become essential as the cell size shirks and the delay spread of each band varies.

• **Minimum Guard Band between Subbands:** Since guard band between the subbands can be minimized because of the low OOBE, 5G new waveform candidates promise higher spectrum usage than OFDM. In general, zero guard band has been considered at the 3GPP meeting.

• **Special Cases:** The proposed concepts can cover several special cases as a *single waveform multiplexing*. In [8], the OFDM system with scalable subcarrier spacing goes through the subband filter, and then they are mixed into an entire f-OFDM system. The authors in [14] managed to aggregate, with a single radio in the unlicensed bands, multiple subbands, which use different protocols at uplink or downlink. These can also be viewed as a *single waveform multiplexing* of f-OFDM/OFDM.

B. Proposed Waveform Multiplexing Transceiver

In this section, we explain a generalized version of the *waveform multiplexing* systems. For simplicity, we employ two CP based waveform candidates.[1] One is f-OFDM which provides much lower OOBE performance, so it can significantly reduce inter-subband interference. The other is GFDM which divides time-frequency resources into blocks that consist of subsymbols. Only a single CP is required for an entire GFDM symbol, which improves the spectral efficiency of the system. Detailed system parameters are given in Table I. Figure 1 illustrates a block diagram of the proposed *waveform multiplexing*.[2] In the i^{th} subband transmitter, $n_{\text{sc},i} \times M_i$ m-QAM symbols are mapped to the M_i desired time grids and the $n_{\text{sc},i}$ desired frequency grids where m is the modulation order. Each subband uses an appropriate subcarrier filter with N_i size. If f-OFDM is used on the i^{th} subband, the subcarrier filter is a rectangular pulse easily implemented by an inverse fast Fourier transform (FFT) filter where $M_i = 1$ and N_i becomes FFT size. If GFDM is used on the i^{th} subband, each sample passes through a corresponding subcarrier filter. These are time- and frequency-shifted versions of a prototype filter. A CP with $n_{\text{cp},i}$ length, is added to the waveform symbol of the i^{th} subband. Next, it passes through a subband filter, which is a bandpass FIR filter in the f-OFDM case or a coefficient 1 in the OFDM and GFDM case with time domain convolution. Finally, the baseband waveform signals are arranged according to the center frequencies of their subbands. The procedures at the receiver are processed inversely. The GFDM receiver uses a post processing block such as zero-forcing to mitigate inter-carrier interference after subcarrier filtering, while OFDM/f-OFDM does not use this.

In fact, it is necessary to adjust the parameters of the waveforms the proposed *waveform multiplexing*. This is because the sampling rate per subband is the same. The numbers of subcarriers and subsymbols are depending on and limited by a given subcarrier spacing with the fixed sampling rate. Moreover, the main concern with designing a GFDM system

[1] We do not employ FBMC since it do not use CP and has high complexity in the *waveform multiplexing* system.

[2] The proposed *waveform multiplexing* is one of *waveform multiplexing* systems, i.e., any design satisfying the requirements explained in Section II-A could be called as *waveform multiplexing*.

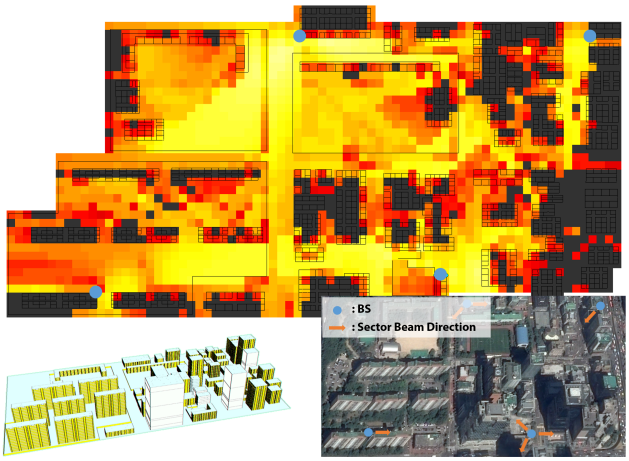

Fig. 2. A urban micro scenario for 3D system-level simulations: (bottom right) a real environment, GangNam Station, Seoul, South Korea; (bottom left) the digital map of GangNam Station in the 3D ray-tracing tool; (top) a color map of measured received powers.

is that the number of subsymbols has to be an odd number so that its transmit filter matrix can be invertible. Note that guard subsymbol is not considered which decrease the spectral efficiency of the GFDM system when M_i is small.

III. 3D Evaluation Environments

In this section, we introduce a 3D channel model and present a realistic environment.

A. Outdoor Scenario

Figure 2 shows the proposed channel environment in an outdoor scenario.[3] We made a digital map of the buildings surrounding GangNam Station, Seoul, South Korea. In 3D space, we deploy 4 micro BSs, which depicts a 7-cell hexagonal layout, more practically while in the 2D conventional model the micro BSs are placed on a regular grid. The coverages of each cell is different due to the varying shapes and heights of the buildings. In addition, the buildings have detailed interiors consisting of glass, metal, concrete, sheetrock, and wood. Such materials possess different attenuation factors. The micro BSs are sectorized into 3 cells with a 3-sector beam antenna so we use the pattern of the Katherine antenna that is typically used in the LTE. Note that the micro BSs are placed at 1.5 m height above the roof of buildings and their inter site distances are approximately 200 m.

B. 3D Channel Generation

The proposed 3D channel model is divided into large scale fading coefficients, power delay profiles (PDPs), and small scale fading coefficients. We measure the received powers and the root mean square (RMS) delays from the BSs to the users using a 3D ray-tracing tool, Wireless System Engineering (WiSE) developed by Bell Laboratories [15]. The received powers are measured at every subcarrier while the RMS delays are measured at the center frequencies of the subbands. Then,

[3]The picture of GangNam Station is taken from the website (http://earth.google.com).

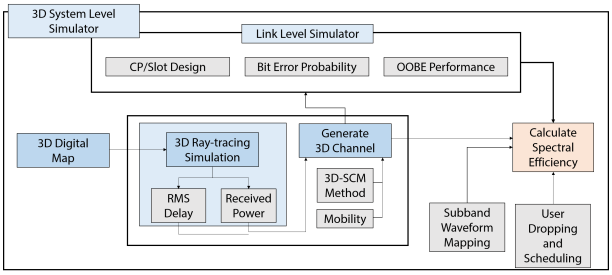

Fig. 3. Block diagram of 3D system-level simulation.

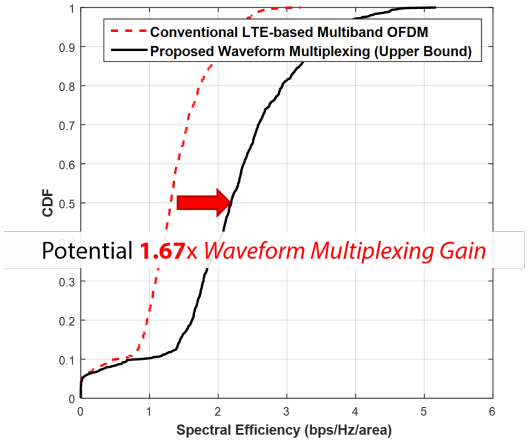

Fig. 4. CDF of the spectral efficiency for the upper bound of the *waveform multiplexing* and the LTE-based multiband OFDM in the urban micro scenario.

we calculate large scale fading per subcarrier of the users from the received powers.

The PDPs are modeled by methods adopted from 3GPP 3D spatial channel model (SCM) [16]. To apply 3D-SCM to the 3D digital map, we approximate the distribution of WiSE output (non-exponential distribution) to that of 3D-SCM (exponential distribution) with appropriate log mean ($\mu_{\text{DS},i}$) and log variance ($\xi_{\text{DS},i}$) of the delay spread on the i^{th} subband. We set this to

$$F_T(\tau_{\text{RMS},i}) \overset{d}{\approx} F_T(\tau_{\text{RMS,WiSE},i})$$

where $F_X(x)$, $\tau_{\text{RMS},i}$, $\overset{d}{\approx}$, and $\tau_{\text{RMS,WiSE},i}$ denote CDF of a random variable x, generated RMS delay spread on the i^{th} subband, approximation in CDF, and measured RMS delay spread from WiSE on the i^{th} subband, respectively. We generate delays using the 3D-SCM method as

$$\tau'_{j,i} = -r_\tau \sigma_{\tau,i} \ln(X_j),\ \tau_{j,i} = \text{sort}\left(\tau'_{j,i} - \min(\tau'_{j,i})\right)$$

where $\sigma_{\tau,i} = 10^{(\tilde{s}\xi_{\text{DS},i}+\mu_{\text{DS},i})}$, $\tilde{s} \sim \mathcal{N}(0,1)$, $X_j \sim \mathcal{U}(0,1)$, $r_\tau = 2.2$ and cluster index $j = 1, 2, 3, ..., J$ ($J = 20$). Then, the cluster powers are given by

$$P'_{j,i} = \exp(\tau_{j,i}\frac{r_\tau - 1}{r_\tau \sigma_\tau})10^{\frac{-Z_{j,i}}{10}},\ P_{j,i} = \frac{P'_{j,i}}{\sum_{j=1}^{J} P'_{j,i}}$$

where $Z_j \sim \mathcal{N}(0,4)$ is the per cluster shadowing term in dB. As a result, $\tau_{\text{RMS},i}$ can be calculated from the terms, $\tau'_{j,i}$ and $P_{j,i}$.

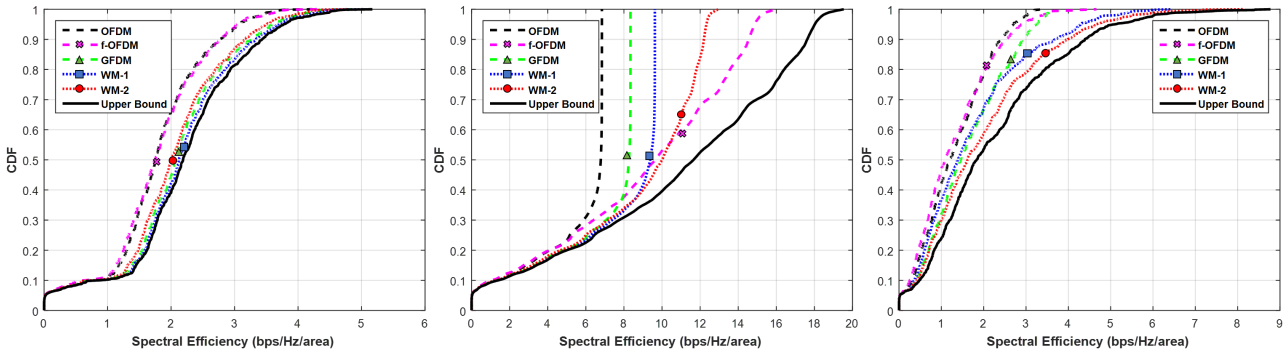

Fig. 5. Performance comparisons of *waveform multiplexing* sets: (a) CDF of the spectral efficiency for *waveform multiplexing*; (b) CDF of the spectral efficiency assuming no intercell interference; (c) CDF of the spectral efficiency of the edge subcarriers.

TABLE I. SYSTEM PARAMETERS

Sampling Rate per Subband (MHz)	34.56		
System Bandwidth (MHz)	51.84		
Center Frequency (GHz)	5		
Transmit Power of the Micro BS (dBm)	49 [16]		
Maximum Height of the Users	32.5 (on the 9th floor) [16]		
Noise Floor (dBm/Hz)	-174		
Backoff Calibration (dB)	5		
Subband Index	1st	2nd	3rd
Subcarrier Spacing (kHz)	67.5	16.875	130
Number of Subcarriers (K_i)	512	2048	256
Number of Allocated Subcarriers ($n_{\mathrm{SC},i}$)	256	1024	128
Subband Bandwidth (MHz) (Δ_i)	17.28	17.28	17.28
Center Frequency of Subband (GHz) (F_i)	4.98272	5.00000	5.01728
CP length ($n_{\mathrm{CP},i}$)	71	76	73
Subband filter Order (L_i)/Number of Subsymbols (M_i)			
OFDM Set	0/1	0/1	0/1
f-OFDM Set	256/1	1024/1	128/1
GFDM Set	0/3	0/1	0/7
WM-1	0/3	1024/1	0/7
WM-2	256/1	1024/1	0/7

Lastly, we assume small-scale fading coefficients are complex Gaussian random variables with zero mean and unit variance. Note that the proposed 3D channel model is realistic, since large scaling fading, OOBE propagations per subcarrier and PDPs are derived from the realistic environment and outputs of the 3D ray-tracing tool.

IV. PERFORMANCE EVALUATION

In this paper, we present the *waveform multiplexing* of three subbands. In considering a downlink system, we assume perfect channel estimation, frequency localization and time synchronization to evaluate the best performance. We organize a total of 5 sets, made up of 3 *single waveform multiplexing* sets and 2 *waveform multiplexing* sets. As the *single waveform multiplexing* set, we arrange (i) OFDM, (ii) f-OFDM, and (iii) GFDM with filter modifications, all of which have 3 subbands with different subcarrier spacings. We also arrange a waveform set, (iv) {GFDM, f-OFDM, GFDM} with a subband set, {the 1st subband, the 2nd subband, the 3rd subband}, which is denoted as a *waveform multiplexing* set-1 (WM-1). We arrange another set, denoted as *waveform multiplexing* set-2 (WM-2) as follows, (v) {f-OFDM, f-OFDM, GFDM}.

A. Simulation Procedure

We investigate the data rate performance of the proposed *waveform multiplexing* sets. We assume that the BSs and the users are connected with point-to-point communication in a full buffer traffic scenario. The mobility of the users could have no effect on system performance (spectral efficiency) due to perfect channel estimation, so we assume the mobilities of all users to be zero. The users are uniformly distributed on the ground and on every floor of the buildings, which are randomly scheduled by the associated BS that provides the strongest SNR. The users who require a long symbol duration such as LTE applications are supported on the 2nd subband, while the users requiring a short symbol duration, for example URLLC, and the in-between applications are serviced on the 3rd and the 1st subbands, respectively. We also assume that guard bandwidth is 0 Hz. The other system overhead are given by the overhead of the reference, common channels, synchronization, and physical broadcast channel = 4, 17, 0.29, and 0.28 percent, which are based on the LTE overhead.

In the f-OFDM system, we assume the transmitter use FIR bandpass filters of soft-truncated-sinc-function with the raised-cosine window and with 2.5 guard tones defined in [17]. In the GFDM system, the transmitter uses root-raised-cosine prototype filters with 0.1 of rolloff factor and the receiver uses a zero-forcing filter. We assume that one slot for each subband– the basic unit of the subframe at downlink– consists of 8 OFDM/f-OFDM symbols, similar to the LTE system. Similarly, one slot of GFDM for the 1st, the 2nd, and the 3rd subbands consists of 9, 8, and 7 subsymbols (3, 8, and 1 symbols), respectively. From the slot organization, we recognize that each waveform has a different CP overhead.

Figure 3 illustrates the procedure for the 3D system-level simulations. We first generates the 3D channels as noted in Section III. The dynamic CP lengths are determined from the maximum delay spread for each subband. At the link-level simulator, we measure the probability of bit error of the waveforms under the generated 3D channels. We also evaluate the OOBE performance of the waveforms on each subband. Finally, we calculate spectral efficiency by combining measurements such as SINR, the probability of bit error, OOBE, and so on.

B. Waveform Multiplexing Gain

Prior to the system-level simulation, we verify how much the proposed *waveform multiplexing* gains we can achieve compared to the conventional system. We assume the *waveform multiplexing* has zero guard band, the optimal CP length per subband, and zero OOBE so that it can be considered as the upper bound of every *waveform multiplexing* set. We also assume that the conventional system employs LTE-based multiband OFDM with 10 percent guard band, the LTE CP length and -35 dB OOBE (not measured data). Figure 4 illustrates the potential gain of the *waveform multiplexing* in the urban micro environment. We confirm that the proposed *waveform multiplexing* has 1.67 times larger gain than the conventional system at the median cumulative density function (CDF).

C. System-level Simulation Result

Figure 5 shows that the system-level performance comparisons of the *waveform multiplexing* sets. In the urban micro environment, the performance of the sets of GFDM, WM-1, and WM-2 are close to the upper bound of the proposed *waveform multiplexing* as shown in Fig. 5(a). This is because that the CP overhead significantly affects on the spectral efficiency and the symbol transmit power, while the influence of the interference from the OOBE is less than that from the intercell (interference limited environments). In contrast, Fig. 5(b) shows that f-OFDM exhibits the best performance assuming no intercell interference (noise limited environment) due to the lower OOBE. WM-1 and WM-2 could, nonetheless, still serve as good options, considering how impractical too many high-order QAM techniques are. Figure 5(c) illustrates that WM-1 and WM-2 outperform the others at the edge subcarriers (2 subcarriers per subband near the adjacent subband) in the interference limited environment. Note that the *waveform multiplexing* with multiple waveforms could have a better spectrum usage than the *single waveform multiplexing* schemes by choosing a efficient waveform for each subband. From the evaluation results, we confirm that the systems consisting of different waveforms have better performance than the systems based on a single waveform.

V. Conclusion

This paper has presented a potential of a system that consists of different waveforms on each numerology, which is a waveform subband system operated on one frequency band. We have named this concept *waveform multiplexing*. To support various applications for 5G, the *waveform multiplexing* possesses three characteristics including multiplexing of waveforms on subbands with scalable subcarrier spacing, dynamic CP, and minimum guard band. Based on the 3D ray-tracing evaluation under the realistic environment, GangNam Station, and the proposed 3D channel, we have evaluated the system-level performances of the proposed *waveform multiplexing*. The performances vary in a certain environment according to both the OOBE and the time overhead of the waveform candidates. From the results, we have confirmed that the *waveform multiplexing*, which consists of different waveforms on subbands, have strong potential in the system of frequency multiplexing of numerologies. In future work, we will investigate agile spectrum-sharing by utilizing the proposed *waveform multiplexing* and uplink *waveform multiplexing*. Considering more subband filtering and windowing techniques will also be our future work.

Acknowledgment

This research was supported by the MSIP (Ministry of Science, ICT and Future Planning), Korea, under the "IT Consilience Creative Program" (IITP-2017-0-01015) supervised by the IITP (Institute for Information & Communications Technology Promotion) and ICT R&D program of MSIP/IITP (2015-0-00300).

References

[1] G. Wunder, P. Jung, M. Kasparick, T. Wild, F. Schaich, Y. Chen, S. T. Brink, I. Gaspar, N. Michailow, A. Festag, L. Mendes, N. Cassiau, D. Ktenas, M. Dryjanski, S. Pietrzyk, B. Eged, P. Vago, and F. Wiedmann, "5GNOW: non-orthogonal, asynchronous waveforms for future mobile applications," *IEEE Commun. Mag.*, vol. 52, no. 2, pp. 97–105, Feb. 2014.

[2] D. Gesbert, M. Kountouris, R. W. Heath, Jr., C.-B. Chae, and T. Salzer, "Shifting the MIMO paradigm: From single user to multiuser communications," *IEEE Sig. Proc. Mag.*, vol. 24, no. 5, pp. 36–46, Oct. 2007.

[3] Y.-G. Lim, C.-B. Chae, and G. Caire, "Performance analysis of massive MIMO for cell-boundary users," *IEEE Trans. Wireless Commun.*, vol. 14, no. 12, pp. 6827–6842, Dec. 2015.

[4] M. Chung, M. Sim, J. Kim, D.-K. Kim, and C.-B. Chae, "Prototyping real-time full duplex radios," *IEEE Commun. Mag.*, vol. 53, no. 9, pp. 56–64, Sep. 2015.

[5] Y. Saito, Y. Kishiyama, A. Benjebbour, T. Nakamura, A. Li, and K. Higuchi, "Non-orthogonal multiple access (NOMA) for cellular future radio access," in *Proc. IEEE VTC Spring*, June 2013, pp. 1–5.

[6] H. Kim, Y.-G. Lim, C.-B. Chae, and D. Hong, "Multiple access for 5G new radio: Categorization, evaluation, and challenges," *arXiv preprint arXiv: 1703.09042*, Mar. 2017.

[7] T. Kwon, Y.-G. Lim, B. Min, and C.-B. Chae, "RF lens-embedded massive MIMO systems: Fabrication issues and codebook design," *IEEE Trans. Microw. Theory Tech.*, vol. 64, no. 7, pp. 2256–2271, July 2016.

[8] X. Zhang, M. Jia, L. Chen, J. Ma, and J. Qiu, "Filtered-OFDM - enabler for flexible waveform in the 5th generation cellular networks," in *Proc. IEEE Globecom*, Dec. 2015, pp. 1–6.

[9] J. Abdoli, M. Jia, and J. Ma, "Filtered OFDM: A new waveform for future wireless systems," in *Proc. IEEE Int. Workshop on SPAWC*, June 2015, pp. 66–70.

[10] N. Michailow, M. Matth, I. S. Gaspar, A. N. Caldevilla, L. L. Mendes, A. Festag, and G. Fettweis, "Generalized frequency division multiplexing for 5th generation cellular networks," *IEEE Trans. Commun.*, vol. 62, no. 9, pp. 3045–3061, Sept. 2014.

[11] B. Farhang-Boroujeny, "OFDM versus filter bank multicarrier," *IEEE Sig. Proc. Mag.*, vol. 28, no. 3, pp. 92–112, May 2011.

[12] ITU-R Rep. M.2135-1, *Guidelines for evaluation of radio interface technologies for IMT-Advanced*, Dec. 2009.

[13] J. Jang, M. Chung, H. Hwang, Y.-G. Lim, H. Yoon, T. Oh, B. Min, Y. Lee, K. Kim, C.-B. Chae, and D.-K. Kim, "Smart small cell with hybrid beamforming for 5G: Theoretical feasibility and prototype results," *IEEE Wireless Commun. Mag.*, vol. 23, no. 6, pp. 124–131, Dec. 2016.

[14] S. Hong, J. Mehlman, and S. Katti, "Picasso: flexible RF and spectrum slicing," in *Proc. ACM SIGCOM*, Oct. 2012, pp. 37–48.

[15] R. Valenzuela, D. Chizhik, and J. Ling, "Measured and predicted correlation between local average power and small scale fading in indoor wireless communication channels," in *Proc. IEEE VTC Spring*, vol. 3, May 1988, pp. 2104–2108.

[16] 3GPP TR 38.873 V12.2.0, *Study on 3D channel model for LTE*, June 2015.

[17] 3GPP R1-165425, "f-OFDM scheme and filter design," *Huawei, HiSilicon*, May 2016.